Available online at www.sciencedirect.com
ScienceDirect
Ceramics International 38 (2012) 55–63
CERAMICS INTERNATIONAL
www.elsevier.com/locate/ceramint

The role of strontium and potassium on crystallization and bioactivity of Na_2O–CaO–P_2O_5–SiO_2 glasses

S.M. Salman *, S.N. Salama, H.A. Abo-Mosallam

Glass Research Dept., National Research Centre, El-Behoos St. Dokki, Cairo, Egypt

Received 1 March 2011; received in revised form 24 May 2011; accepted 17 June 2011
Available online 24th June 2011

Abstract

The effect of SrO/CaO and K_2O/Na_2O replacements on the crystallization process of glasses based on Na_2O–CaO–P_2O_5–SiO_2 system was investigated. The glasses were thermally treated through controlled heat treatment regimes to obtain glass ceramic materials. Combeite $Na_2Ca_2Si_3O_9$, sodium calcium silicate $Na_2Ca_3Si_6O_{16}$, wollastonite solid solution, and whitlockite $Ca_3(PO_4)_2$ were identified as major crystalline phases in the prepared thermally treated glasses. No potassium and strontium-containing phases could be detected in the glass–ceramics; potassium seems to be accommodated in the wollastonite structure, while strontium might be incorporated in the sodium calcium silicate structure.

The surface reactivity of the prepared glass–ceramic specimens was also studied *in vitro* in Kokobo's simulated body fluid (SBF). EDAX, SEM, inductively coupled plasma ICP, and FTIR were used to examine the formation of apatite layer's surface and characterize the glass ceramic surface and SBF compositional changes. A decrease in the bioactivity of the glass ceramic was observed as Na_2O was replaced by K_2O. Strontium together with calcium ions in the apatite layer formed was detected with SrO/CaO replacement.

The role played by the glass oxide constituents in determining the crystallization and bioactivity behaviour of the prepared thermally treated glasses was discussed.

Keywords: Crystallization; Glass–ceramics; SBF; Bioactivity; Strontium; Potassium

1. Introduction

Variety of bioactive glasses and glass ceramics are used for biomedical applications such as dental, orthopedic, and maxillopacial [1]. Bioactive glasses and glass–ceramics are widely studied due to their particular property of directly bonding to the human bones through the formation of biologically active apatite layer at the bone/implant interface [2]. Bioceramics have received special interest due to their unique characteristics, including (i) a rapid rate of surface reaction that leads to their direct attachment to bone via a chemical bond [3]; (ii) their relatively low softening temperature that can be used as a sintering aid to bond the ceramic particles and fill the micro pores during the sintering process; (iii) the ease of compositional design with properties specific to particular clinical applications; and (iv) their excellent controllability over a wide range of chemical properties and rate of bonding with tissues [4].

Bioglass®, belonging to the Na_2O–CaO–P_2O_5–SiO_2 system, was the first glass able to form an interfacial bond with living bone after implantation [5]. Since then, more complex compositions have been designed to enhance the bioactivity of the material. Controlled nucleation and crystallization of the glass ceramics in the system Na_2O–CaO–P_2O_5–SiO_2 led to formation material displayed a high mechanical strength and good implantation results [6]. Clupper and Hench [7] carried out quantitative investigations on the effect of crystallinity on the apatite formation on Bioglass® surfaces in vitro. They found that the crystal phase $Na_2Ca_2Si_3O_9$ slightly decreased the formation kinetics of an apatite layer on the Bioglass® sample surface but it did not totally suppress the formation of such layer. Peitl et al. [8] discussed the crystallization tendency of 45S5 bioglass. The study showed that, during the crystallization of the glasses, phosphate ions have been reported to stay in solid solution in the structure of $Na_2Ca_2Si_3O_9$ crystal phase.

A variety of bioglass and bioglass–ceramic materials incorporating modifiers such as strontium were reported.

* Corresponding author.
E-mail address: s.moghazy@yahoo.com (S.M. Salman).

0272-8842/$36.00
doi:10.1016/j.ceramint.2011.06.037

Strontium exhibits clearly beneficial biologically, specifically for healthy bone growth [9]. The essential characteristics and the role of strontium in bone mineral are (i) its specific role in osteoporosis; (ii) its equal share with ionic calcium in the physiological pathway; and (iii) it can be deposited into the mineral structure of bone [10]. Wu et al. [11] reported that the incorporation of Sr ions into $CaSiO_3$ improved the physical and biological properties as compared with that of pure $CaSiO_3$ ceramics. The presence of potassium oxide seems to help the usage of the bioactive glasses, without damaging their thermo-mechanical performances and their bioactivity [12]. Arstila et al. [13] succeeded in synthesized highly bioactive glass–ceramic with composition $6Na_2O$–$11K_2O$–5MgO–22CaO–$1B_2O_3$–$2P_2O_5$–$53SiO_2$.

The purpose of this article is to study the crystallization characteristics and in vitro bioactivity behaviour of the Na_2O–CaO–P_2O_5–SiO_2 glass modified by SrO/CaO and K_2O/Na_2O replacements. The relationship between crystalline phases formed, and bioactivity of the glass–ceramics formed has been concerned.

2. Experimental and methods

2.1. Glass preparation

Glasses were prepared in five different compositions by taking the starting materials as reagent grade ammonium dihydrogen phosphate ($(NH4)H_2{\cdot}PO_4$), calcium carbonate ($CaCO_3$), sodium carbonate (Na_2CO_3), potassium carbonate (K_2CO_3), strontium carbonate ($SrCO_3$), and quartz (SiO_2) in the required stoichiometric ratio in mole% (Table 1). The glasses were prepared by melting the starting materials, in a Pt–2% Rh crucible at 1200–1350 °C in air for 2 h to ensure homogeneity. The melt was cast as rods and buttons, which were then properly annealed at 450–500 °C for 1 h and left to cool down slowly overnight inside the muffle furnace to minimize the strain.

2.2. Differential thermal analysis (DTA)

The thermal behaviour of the finely powdered glass samples was examined using a SETARAM Labsys ™TG-DSC16. The powdered samples were heated in Pt-holder against another Pt-holder containing Al_2O_3 powder as a standard material. A uniform heating rate of 10 °C/min was adopted up to the appropriate temperature of the glasses.

Table 1
Chemical compositions of the investigated glasses.

Sample No.	Oxide constitutions (mole%)					
	Na_2O	K_2O	CaO	SrO	P_2O_5	SiO_2
G_1	12	–	36	–	4	48
G_2	9	3	36	–	4	48
G_3	6	6	36	–	4	48
G_4	12	–	33	3	4	48
G_5	12	–	30	6	4	48

2.3. Crystallization and glass–ceramic formation

For crystallization, a suitable controlled heat-treatment schedule was applied for each glass to obtain thermally treated glass–ceramic materials of holocrystalline mass with minimum residual glassy phase without deformation. To prepare glass–ceramic materials, thermal treatment of the glasses was carried out at temperature in the region of the main DTA exothermic peak determined for each glass. The glass samples were subjected to double stage heat-treatment regimes. Therefore, at endothermic temperature of each glass composition, the glass sample was soaked for 5 h and then the temperature was raised up to the exothermic temperature specific for each glass for 10 h. A heating rate of 10 °C/min was used during the double stage heat-treatment regimes. After crystallization, each sample the muffle furnace was switched off and the samples were allowed to cool down to room temperature.

2.4. X-ray diffraction (XRD)

The X-ray powder diffraction patterns were used to identify the crystalline phases formed in the thermally treated glasses using Bruker AXS D8 Advance X-ray diffractometer (40 kV, 20 mA) from 3° to 80° in steps of 0.01°. The Cu Kα radiation with Ni filtered is used for X-ray analysis. The reference data for the interpretation of the X-ray diffraction patterns was obtained from JCPDS X-ray diffraction card files.

2.5. Scanning electron microscopy (SEM)

The crystallization characteristics and internal microstructures of fractured surfaces of the glass–ceramic samples, coated with gold spray, were examined by using scanning electron microscopy. Representative electron micrographs were obtained by using Philips XL 30 on Electron Probe Microanalyzer.

2.6. Bioactivity (in vitro test)

In in vitro bioactivity test, the selected thermally treated glass i.e. (glass–ceramic) specimens were cut by a low speed diamond disc into rectangular pieces of dimensions (10 mm × 10 mm × 5 mm). These samples were polished and sequentially washed with distilled water in an ultrasonic cleaner and then air-dried. The glass–ceramics were vertically mounted on a nylon string to avoid the deposition of apatite layer by gravity. All the studied samples were soaked at 37 ± 0.5 °C, for 7, 14 and 21 days in 50 mL in Tris-buffered simulated body fluid (SBF) solution. The preparation of SBF was carried out according to the method proposed by Kokubo et al. [3]. The reagents shown in Table 2 were added, in order, to deionized water to make one litre of SBF. The solution was buffered to pH 7.4 with Tris–(hydroxymethyl)-aminomethan $[(CH_2OH)_3CNH_3]$ and hydrochloric acid. The glass–ceramics samples were removed from the SBF, and dried at room temperature. The surfaces of dried samples were analyzed by FTIR and (SEM–EDX) to detect the appearance of HCA layer.

Table 2
Reagents for the preparation of SBF& ionic concentration comparison.

Order	Reagent	Amount (g/L)	Ion	Concentrations (mM)	
				SBF	Blood plasma
1	NaCl	7.996	Na^+	142.0	142.0
2	$NaHCO_3$	0.350	HCO_3^-	4.2	27.0
3	KCl	0.224	K^+	5.0	5.0
4	$K_2HPO_4{\cdot}3H_2O$	0.228	HPO_4^{2-}	1.0	1.0
5	$MgCl_2{\cdot}6H_2O$	0.305	Mg^{2+}	1.5	1.5
6	1 N HCl	~35 mL	Cl^-	147.8	103.0
7	$CaCl_2{\cdot}2H_2O$	0.368	Ca^{2+}	2.5	2.5
8	Na_2SO_4	0.071	SO_4^{2-}	0.5	0.5
9	$(CH_2OH)CNH_2$	6.057	pH at 37 °C	7.40	7.40
10	1 N HCl	~5 mL			

The variation of ion concentrations in the (SBF) solution after soaking the sample was monitored by using inductive coupled plasma (ICP).

2.6.1. Scanning electron microscopy with energy dispersive X-ray analysis (SEM–EDX)

The deposited layers formed on the surface were subsequently examined by (SEM–EDX) using SEM Model Philips XL 30 attached with X-ray unit, with accelerating voltage 30 kV, magnification 10× up to 400 000× and resolution for W (3.5 nm). The samples were coated with carbon.

2.7. Fourier transform infrared (FTIR)

The glass–ceramic samples were analyzed by Fourier-transform infrared spectroscopy before and after exposure to the SBF solution to detect the formation of hydroxyapatite on the surfaces. The reflection angle was set at 758 for the prepared glass–ceramics samples were obtained using the FT-IR-6100 type A machine (The Netherlands). The spectra were obtained between 400 and 2000 cm^{-1} wave number, with resolution of 2 cm^{-1}.

2.8. Inductive coupled plasma

The variation of ion concentrations in the (SBF) solution after soaking the sample was monitored by using inductive coupled plasma model (Jobian Yvon Horiba Ultima 2000). The changes in pH of the SBF solution as a function of time were monitored using a pH meter (Hanna 8417). Each pH value reported is the mean of four measurements performed at each recording time.

3. Results and discussion

3.1. Crystallization characteristics

The crystallization process of the glass during the reheating process (i.e. thermal treatment) is known to be connected to the nature and proportions of the glass oxide constituents. The ability of some cations to build glass forming units or to be housed as modifiers in interstitial positions in the glass structure must also be considered [14]. The DTA data of the glasses (Fig. 1) showed endothermic peaks in the 615–657 °C temperature range. These endothermic peaks are to be attributed to the glass transition (T_g), at which the atoms begin to arrange themselves in preliminary structural elements subsequent to crystallization. One exothermic peak, which is detected in each glass, indicating crystallization reaction in the glasses, is also recorded.

The addition of K_2O at the expense of Na_2O in the base glass G_1, led to the shift of both the endothermic and exothermic peak temperatures towards higher temperature values, i.e. a higher energy is needed to induce crystallization in the thermally treated glass.

Meikhail [15] reported that the addition of potassium instead of sodium in the sodium borate glass led to increasing the activation energy to reach a maximum value of 32.5 kcal/mole for $K_2O/Na_2O = 1$

The glass transition temperatures (T_g) slightly decreased by the addition of SrO at the expense of CaO in the G_4 and G_5 glasses as compared with that of the base glass G_1; This could be attributed to the fact that increased disruption of the glass network may be due to the presence of the slightly larger strontium cation, as well as due to the weaker strontium–oxygen bond strength [9].

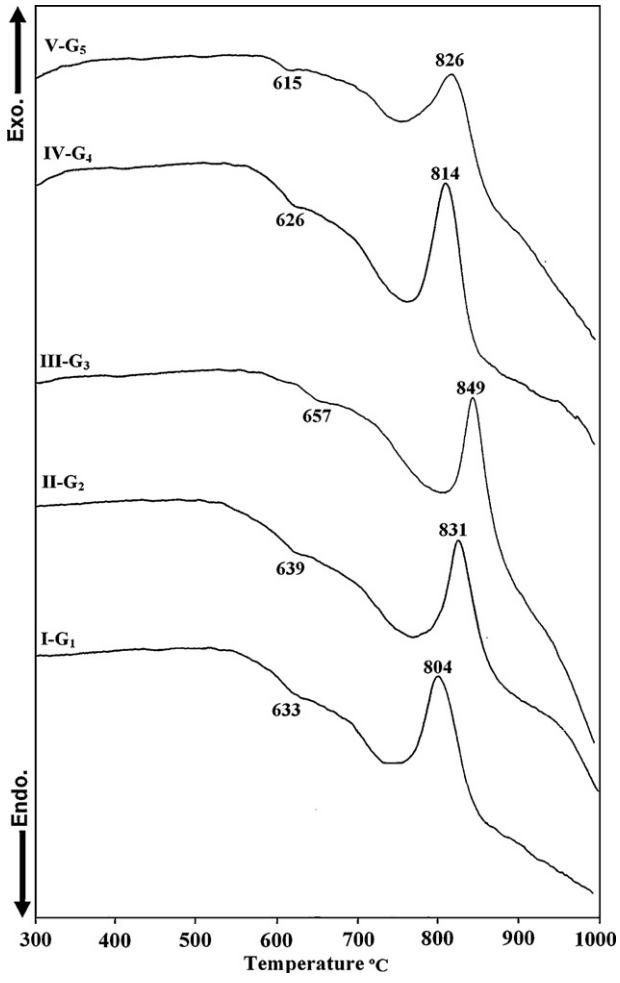

Fig. 1. DTA data of the investigated glasses.

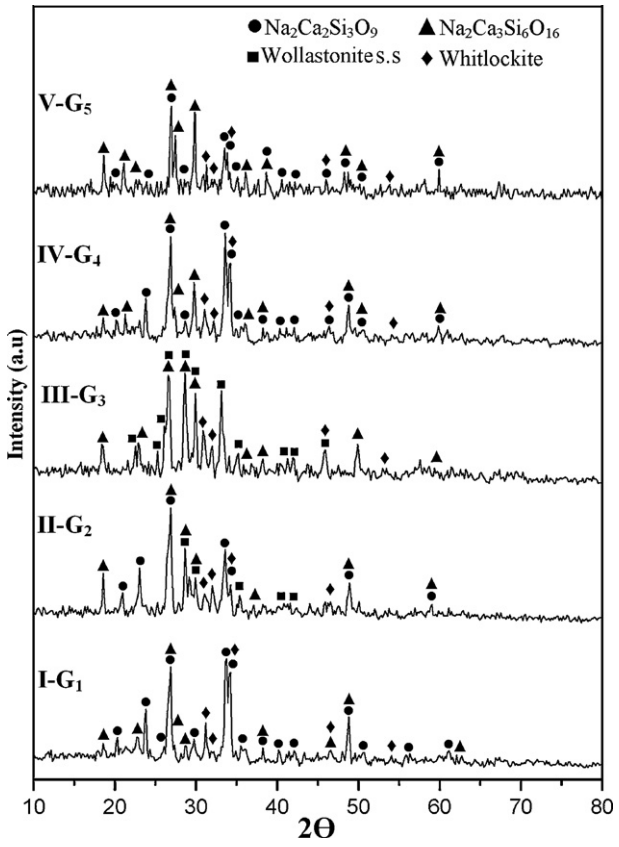

Fig. 2. XRD analysis of crystallized glasses.

The occurrence of the various phases formed in the prepared thermally treated glasses was a function of base composition of the glasses and the thermal treatment parameters used. The X-ray diffraction patterns of the glass–ceramic samples are shown in Fig. 2. Three major crystalline phases, such as combeite [$Na_2Ca_2Si_3O_9$, JCPDS file no. 22-1455], sodium calcium silicate [$Na_2Ca_3Si_6O_{16}$, JCPDS file no. 23-0671], and whitlockite [$Ca_3(PO_4)_2$, JCPDS file no. 09-0169] were identified in the thermally treated base glass G_1. Combeite, as the major phase together with fluoroapatite, was identified by Abo-Mosallam et al. [16] during the crystallization of glass containing SiO_2 38.15, P_2O_5 10.55, Na_2O 13.1, CaO 36.26, and CaF_2 1.94 (in wt%). Whitlockite, is essentially a slowly degrading bioresorbable calcium phosphate ceramic (CPC) and is a promising material in the field of biomedical applications. It has also been observed to have significant biological affinity and activity and to respond very well to the physiological environments [17].

At low K_2O/Na_2O, i.e. G_2, predominant sodium calcium silicate [$Na_2Ca_3Si_6O_{16}$], combeite [$Na_2Ca_2Si_3O_9$], whitlockite [$Ca_3(PO_4)_2$], and wollastonite solid solution [$CaSiO_3$, JCPDS file no. 29-372] phases were developed as indicated from the XRD analysis (Fig. 2, Pattern II). On further increasing of K_2O/Na_2O replacement i.e. G_3 the X-ray diffraction analysis revealed that, wollastonite solid solution phase was developed at the expense of $Na_2Ca_3Si_6O_{16}$ while $Na_2Ca_2Si_3O_9$ phase could not be detected. Arstila et al. [13] reported that the crystal formed in the glass of composition $6Na_2O$–$11K_2O$–$5MgO$–$22CaO$–$1B_2O_3$–$2P_2O_5$–$53SiO_2$ was identified as mono mineralic wollastonite ($CaSiO_3$) phase. In our results, it seems more likely that the potassium could be accommodated in the wollastonite structure.

In case of the thermally treated glasses G_4 and G_5 the partially substitution of SrO at the expense of CaO does not lead to the formation of different phases from those crystallized in glass G_1, however, the $Na_2Ca_3Si_6O_{16}$ phase was increased instead of the combeite $Na_2Ca_2Si_3O_9$ and no strontium containing phases could be detected. This may be attributed to that strontium introduced in the $Na_2Ca_3Si_6O_{16}$ phase.

SEM of the fractured surface shows the effects of K_2O/Na_2O and SrO/CaO replacements on the microstructure of the prepared glass–ceramics (Fig. 3a–c). Fig. 3a shows tiny aggregates of minute crystals formed in the base glass–ceramics G_1, while fine microstructure was obtained by K_2O/Na_2O replacement in the glass–ceramic sample G_3 ((Fig. 3b). However, a globule like structure was formed in the Sr-containig glass–ceramic G_5 (Fig. 3c).

3.2. Bioactivity

Bioactive glasses and glass–ceramics are considered as potential materials for bone substitutes, because they can form a direct bond with the living bone, without the formation of surrounding fibrous tissue. The requirement of a bioactive material is that in the presence of the human physiological environment, a biological active apatite called hydroxyl carbonate apatite layer is produced on their surfaces, which provide the bonding interface with tissues as well as bone [18]. In the present study, the dissolution of the heat treated samples was studied in simulated body fluid with the primary idea of understanding the bioactivity material behaviours in vitro. In biomaterials research, the in vitro studies involving dissolution experiments in solutions similar in composition to those present inside the human body (e.g. simulated body fluid, SBF), have now been recognized as preliminary screening tests on new candidate implant materials [19].

Figs. 4–6 show SEM and EDAX spectra obtained from the glass–ceramic samples before and after soaking in (SBF) solution. The formation of apatite layers on the surfaces of the glass–ceramic samples with different magnitude was sought by using the EDAX-SEM technique after the soaking in the SBF solution for 21 days. Fig. 4a shows apatite layer covered the surface of specimen G_1 after immersion for 21 days in the SBF solution, which was analyzed by EDAX. Fig. 4b shows the EDAX trace from the surface of the base glass–ceramic G_1 before soaking in the SBF solution indicating the presence of Ca, Na, Si, and P. However, EDAX spectra of the G_1 sample after immersion in the SBF solution for 21 days revealed that significant peaks for Ca and P were detected due to the formation of the apatite layer on the surface. Similar formation of Ca–P rich dispersed precipitate is commonly reported to be formed during in vitro leaching treatment of various glass and glass–ceramics materials [20]. Small amounts of magnesium ions were detected in the hydroxyl apatite layer due to the

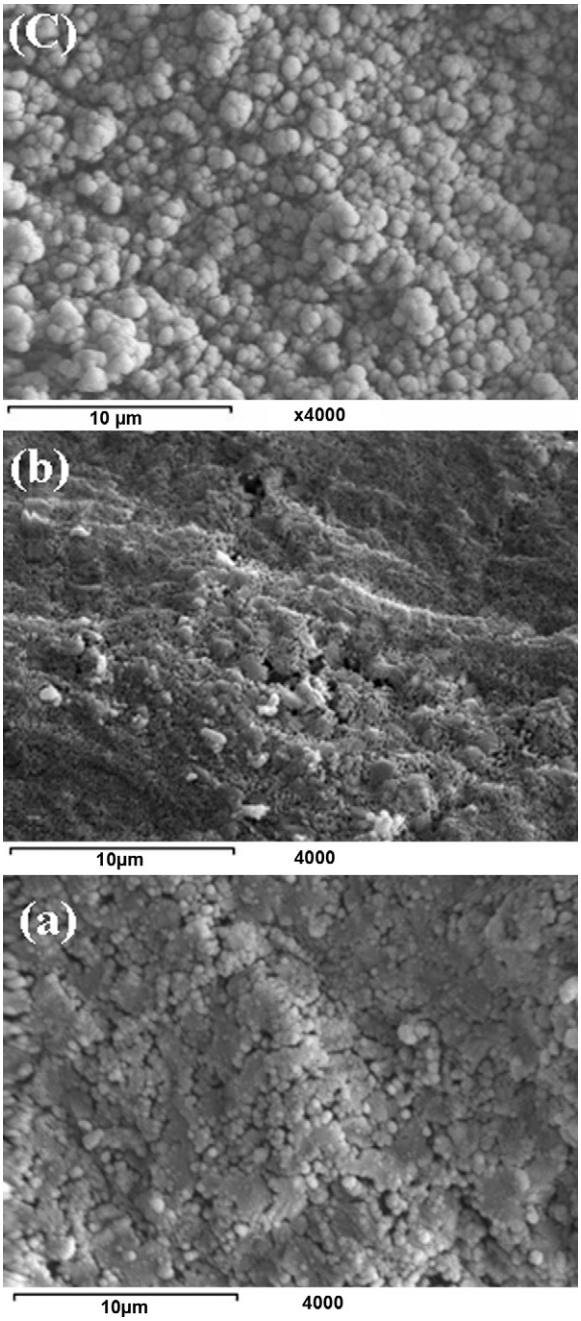

Fig. 3. (a) SEM micrograph of fracture surface of glass–ceramic G_1, (b) SEM micrograph of fracture surface of glass–ceramic G_3 and (c) SEM micrograph of fracture surface of glass–ceramic G_5.

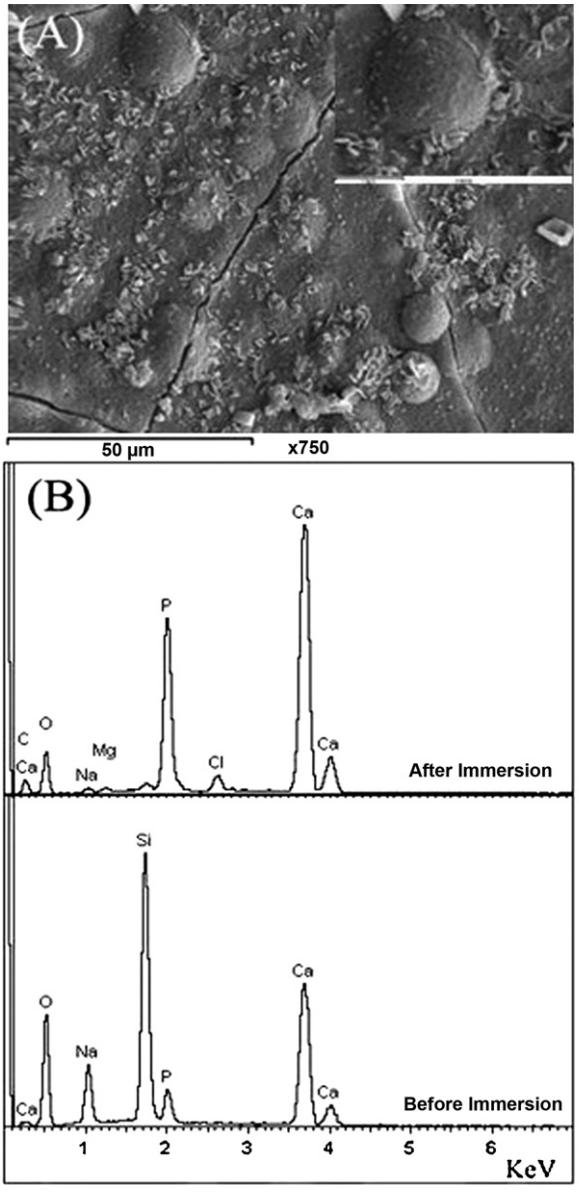

Fig. 4. (a) SEM micrograph of the glass–ceramic surface of specimen G_1 after the immersion in the (SBF) solution (b) EDX of the glass–ceramic surface of specimen G_1 before and after the immersion in the (SBF) solution.

ability of alkaline earth ions to interchange in calcium phosphate crystals lattices [21].

Karlsson and Ylanen [22] reported that the biological behaviour of glasses and glass ceramics depends on the dissolution and the relative proportion of bridging-oxygen bond to non-bridging bond in the phases of the materials, i.e. as the number of non-bridging oxygen bond increased, the bioactivity of the material increased. It is clear that the bioactivity of the $6K_2O/Na_2O$ glass–ceramic sample (i.e. G_3) was lower than that of the base glass–ceramic sample G_1, as indicated from the EDAX patterns (Figs. 4b and 5b, respectively). Fig. 5b revealed that small peak for Si was occurred, i.e. the surface of G_3 sample was not completely covered with apatite layer as compared with that of G_1 (Figs. 4a and 5a, respectively). This may be attributed to the chemical durability of the glass–ceramic sample, which was improved by K_2O/Na_2O replacement. The mixed alkali effect in the glasses leads to lowering the rate of corrosion and increasing the chemical durability [23].

Recent years have witnessed the incorporation of strontium (Sr) into the CaP structure due to its presence in calcified bone. Strontium ions depress bone resorption and maintain bone formation. Therefore, Sr-substituted Ca-phosphate layer is expected to produce enhanced biological and chemical responses in the body [24]. In the present investigation the bioactivity behaviour of the glass–ceramic sample G_5 is still

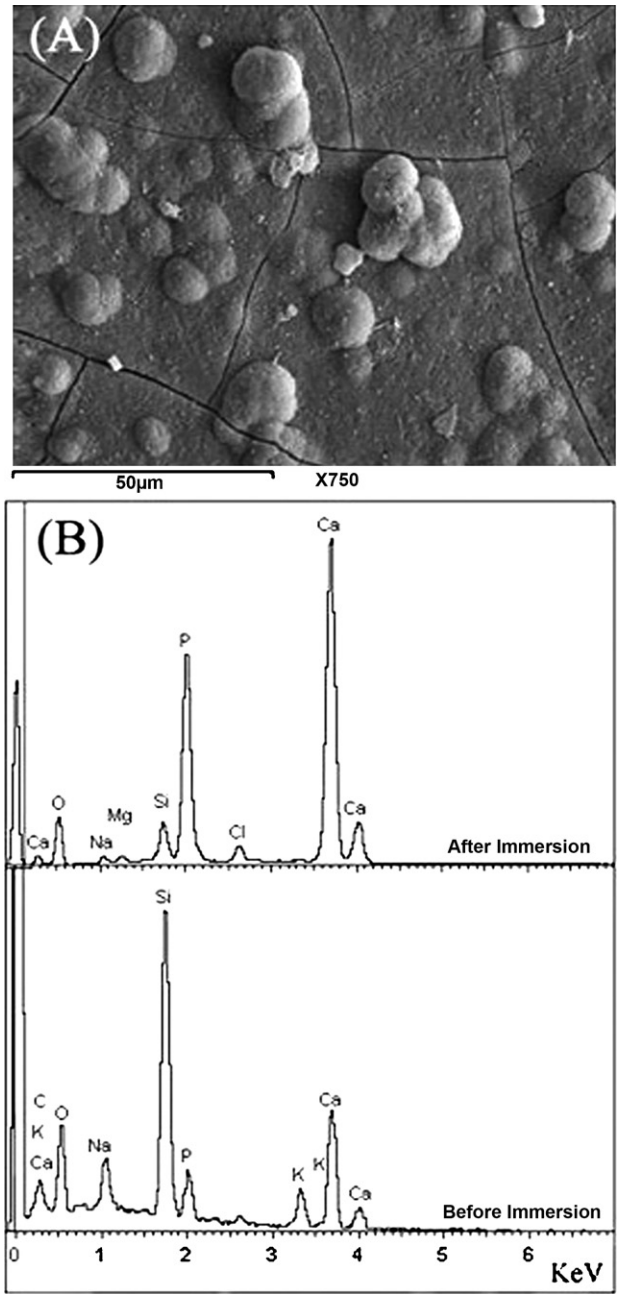

Fig. 5. (a) SEM micrograph of the glass–ceramic surface of specimen G_3 after the immersion in the (SBF) solution (b) EDX of the glass–ceramic surface of specimen G_3 before and after the immersion in the (SBF) solution.

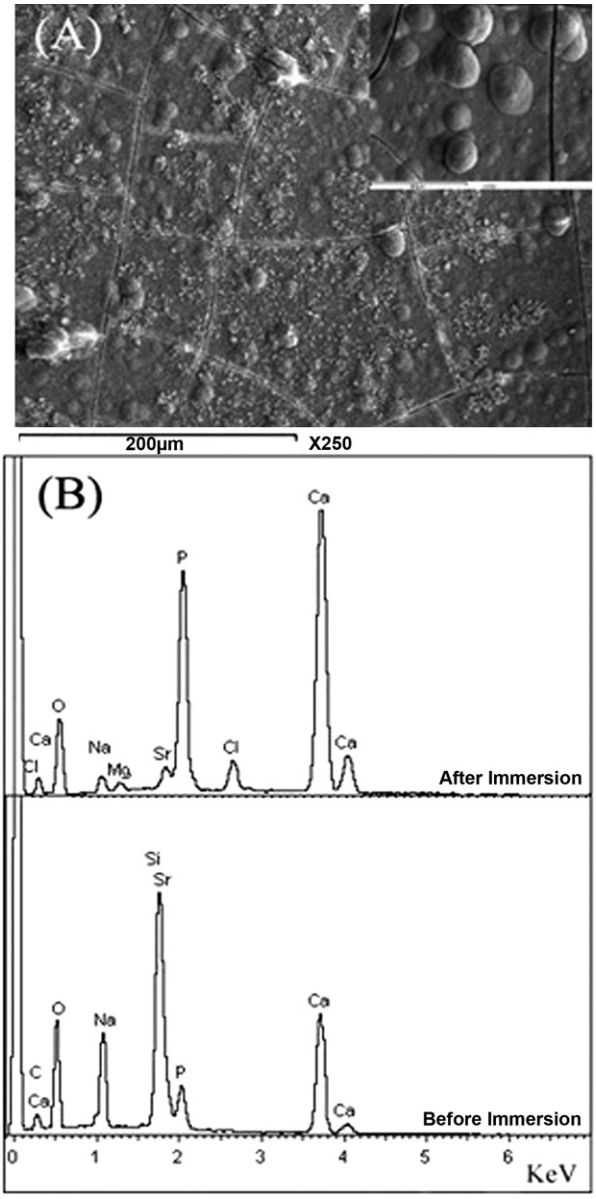

Fig. 6. (a) SEM micrograph of the glass–ceramic surface of specimen G_5 after the immersion in the (SBF) solution (b) EDX of the glass–ceramic surface of specimen G_5 before and after the immersion in the (SBF) solution.

high with SrO/CaO replacements as indicated from the EDAX patterns after soaking in the SBF solution. The EDAX analysis of the surface of the crystalline glass ceramic specimen G_5 after immersion (Fig. 6b) revealed that significant peaks of calcium and phosphorous as well as short peak of strontium were detected. This may be attributed to strontium ions substituted for a part of calcium in hydroxyl apatite layer and form $(Ca,Sr)_5(PO_4)_3(OH)$. Shifting the diffraction lines of apatite phase to higher d-spacing suggests that a solid solution of (strontium/calcium) apatite phase could be formed [9].

The formation of apatite in SBF is strongly pH dependent; the increase in pH actually signifies for the reduction in the concentration of H^+ due to the replacement of metal ions in the glass and subsequent production of OH^- ions due to breaking of siloxane bond [20]. The pH rise in SBF is less pronounced with K_2O/Na_2O replacement in the glass, it might therefore be expected that the deposition of apatite in SBF decreases with the addition of K_2O in the glass (Fig. 7).

Fig. 7 shows ionic concentrations in SBF after immersion of glass ceramic samples for 3 weeks. For all glass–ceramic samples, the concentrations of the phosphate ions decrease compared to the concentration of the initial SBF solution. This may be associated with the apatite layer formation [17]. Peitl et al. [8] reported that the decrease in calcium and phosphorous ion concentrations in the SBF solution indicates the formation, crystallization, and growth of the $CaO–P_2O_5$ rich layer. The glass–ceramic sample G_1, which is formed has represented the

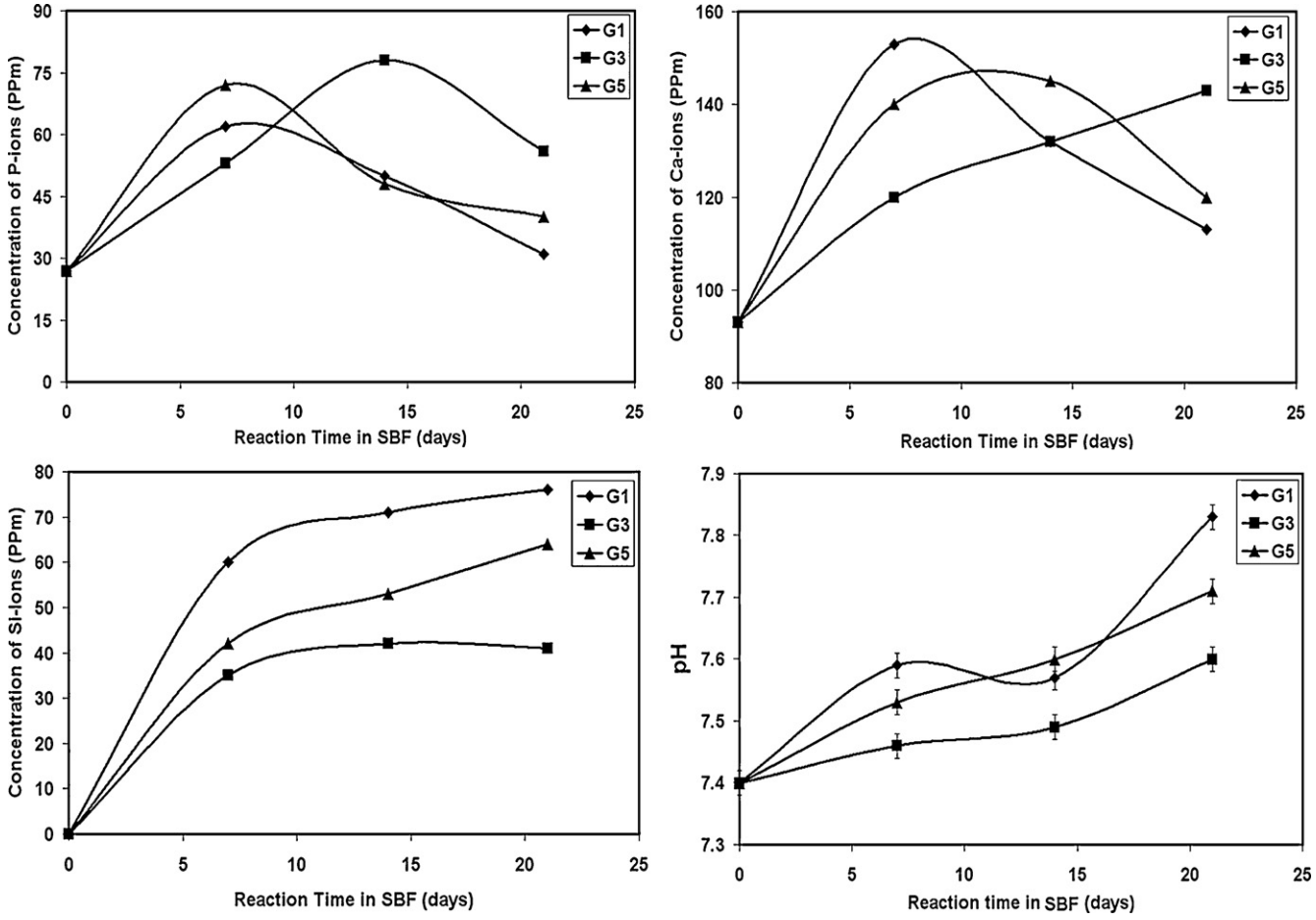

Fig. 7. Ion concentrations and pH value of SBF solution after immersion of glass–ceramic samples for 7, 14 and 21 days.

lowest phosphate concentrations in SBF. On the other hand, the glass–ceramic sample G_3, has given the highest phosphate concentration in SBF after 3 weeks immersion in SBF i.e. the lowest bioactivity. The silicon release from the glass–ceramic has significantly decreased with the potassium addition i.e. G_3. This indicates that the reaction between the glass–ceramic sample and SBF solution was suppressed and the formation of apatite layer was also suppressed.

Furthermore, in order to provide complementary evidences of the apatite layer formation on the glass–ceramics, FTIR spectroscopy was performed on both the virgin surface and the immersed glass–ceramic surface, after 3 weeks in the SBF solution. The difference between the infrared reflection spectra of unreacted bioglass–ceramics and reacted bioglass–ceramic is restricted to the bands between 700 and 400 cm^{-1} which are associated with the formed crystalline phases [25]. The changes in the infrared reflected spectra obtained from the surfaces of the selected glass–ceramic samples G_1, G_3, and G_5 upon immersion in SBF for 21 days and longer in comparison to the spectrum of the unreacted glass–ceramic are shown in Fig. 8a–c, respectively.

FTIR spectra after SBF immersion showed either a single peak or a split peak at approximately 560 cm^{-1}. This is the most characteristic region for apatite and other phosphates, and it corresponds to P–O bonding vibrations in a PO_3^{4-} tetrahedron and indicates the presence of crystalline calcium phosphates including hydroxyl apatite (HA) and hydroxyl carbonate apatite (HCA). A single peak in this region suggests the formation of non apatitic or amorphous calcium phosphate (ACP), which is usually taken as indication to the presence of precursors to hydroxyapatite [26]. Apatitic PO_3^{4-} groups give characteristic split bands at 560 and 600 cm^{-1} [27]. At 3 weeks immersion in the SBF solution (Fig. 8a–c), this split phosphate peak is most clearly pronounced for glass–ceramic samples G_1, G_3, and G_5.

Serra et al. [28] reported that, the spectrum of the reference bioactive glass immersed in SBF shows two bands located at 603 cm^{-1} and 564 cm^{-1} which attributed to P–O bending vibration in the crystalline hydroxyapatite phase. The presence of carbonate substitution in the apatite is indicated by the peak at about 870 cm^{-1} [29], present in immersed glass–ceramic specimens G_1, G_3 and G_5 after 3 week immersion in SBF (Fig. 8)

4. Conclusions

Glass–ceramic materials based on Na_2O–CaO–P_2O_5–SiO_2 glass system modified by SrO/CaO and K_2O/Na_2O replacements were successfully prepared and examined by SBF solution in vitro. Sodium calcium silicate phases and calcium

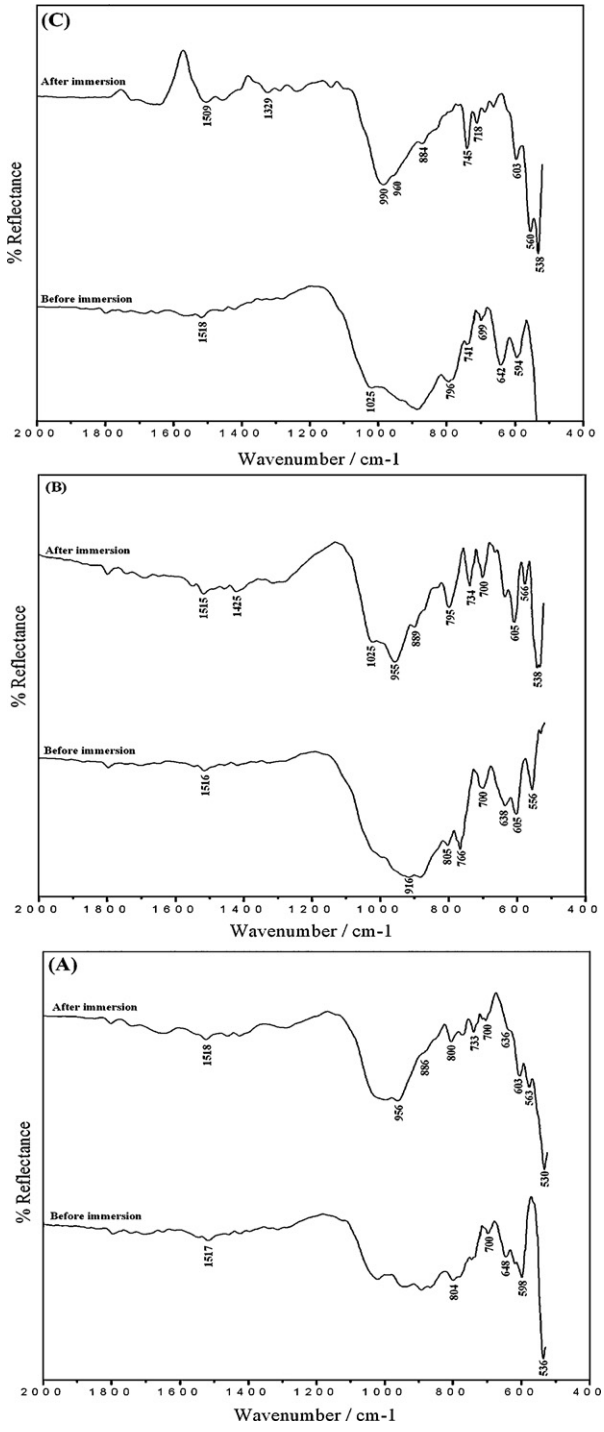

Fig. 8. FTIR of (a) G_1, (b) G_3 and (c) G_5 crystallized samples before and after immersion in SBF solution.

phosphate together with wollastonite solid solution could be formed during the crystallization. Potassium ions could be accommodated in the wollastonite structure while strontium ions might be incorporated in sodium calcium silicate phase. The bioactivity studies on the prepared glass–ceramic samples show that the materials are capable of bonding with the human bone due to the formation of apatite layer after immersion in SBF solution. Our results indicate that K_2O/Na_2O replacement in the glass system has reduced the formation of apatite layer as compared with that of the potassium-free variety.

References

[1] P.J. Ducheyne, Bioceramics: material characteristics versus in-vivo behavior, J. Biomed. Mater. Res. Appl. Biomater. 21A (1987) 219–236.
[2] P.N. De AZa, A.H. De Aza, P. Pena, S. De Aza, Bioactive glass and glass–ceramics, Ceramica y Vidro Bolletin Sociedad Espanola Ceramica 46 (2) (2007) 45–55.
[3] T. Kokubo, T. Kitsugi, T. Yamamuro, Solution able to reproduce in vivo surface-structure changes in bioactive glass–ceramics A-W, J. Biomed. Mater. Res. 24 (1990) 721–734.
[4] T. Yamamuro, Bioceramics, Elsevier, New York, 1995, pp. 123–136.
[5] L.L. Hench, The story of bioglass, J. Mater. Sci.: Mater. Med. 17 (2006) 967–968.
[6] G. Partridge, P.W. Mcmillan, Glass Technol. 15 (1974) 127.
[7] D.C. Clupper, L.L. Hench, Crystallization kinetics of tape cast bioactive glass 45S5, J. Non-Cryst. Solids 318 (2003) 43–48.
[8] O. Peitl, E.D. Zanotto, L.L. Hench, Highly bioactive P_2O_5–Na_2O–CaO–SiO_2 glass–ceramics, J. Non-Cryst. Solids 292 (2001) 115–126.
[9] R.G. Hill, A. Stamboulis, R.V. Law, A. Clifford, M.R. Towler, C. Crowley, The influence of strontium substitution in fluorapatite glasses and glass–ceramics, J Non-Cryst. Solids 336 (2004) 223–229.
[10] C.T. Wong, W.W. Lu, W.K. Chan, K.M.C. Cheung, D.K. Luk, D.S. Lu, In vivo cancellous bone remodeling on a strontium containing hydroxyapatite (Sr-HA) bioactive cement, J. Biomed. Mater. Res. 68A (2003) 513–521.
[11] C. Wu, Y. Ramaswamy, D. Kwik, H. Zreiqat, The effect of strontium incorporation into $CaSiO_3$ ceramics on their physical and biological properties, Biomaterials 28 (2007) 3171–3181.
[12] V. Cannillo, A. Sola, Potassium-based composition for a bioactive glass, Ceram. Int. 35 (2009) 3389–3393.
[13] H. Arstila, L. Hupa, K.H. Karlsson, M. Hupa, Influence of heat treatment on crystallization of bioactive glasses, J. Non-Cryst. Solids 354 (2008) 722–728.
[14] L. Stoch, Structure and crystallization of multi component glasses, apatite structures $Ca_{10}(PO_4)_6F_x(OH)_{2-x}$, in: XIX Pro. Inter. Congr. Glass, Invited Papers, 1–6 July, vol. 1, Edinburgh, Scotland, (2001), pp. 62–73.
[15] M.S. Meikhail, Conduction modeling in mixed alkali borate glasses, Int. J. Pure Appl. Phys. 1 (2005) 191–197.
[16] H.A. Abo-Mosallam, N. Salama, S.M. Salman, Formulation and characterization of glass–ceramics based on $Na_2Ca_2Si_3O_9$–$Ca_5(PO_4)_3F$–Mg_2SiO_4-system in relation to their biological activity, J. Mater. Sci.: Mater. Med. 20 (2009) 2385–2394.
[17] N. Kivrak, A.C. Tas, Synthesis of calcium hydroxyapatite–tricalcium phosphate composite bioceramic powders and their sintering behavior, J. Am. Ceram. Soc. 81 (1998) 2245.
[18] M.A. Sainz, P. Pena, S. Serena, A. Caballero, Influence of design on bioactivity of novel $CaSiO_3$–$CaMg(SiO_3)_2$ biocermics: in vitro simulated body fluid test and thermodynamic simulation, Acta Biomater. 6 (2010) 2797–2807.
[19] S. Roy, B. Basu, In vitro dissolution behavior of SiO_2–MgO–Al_2O_3–K_2O–B_2O_3–F glass–ceramic system, J. Mater. Sci.: Mater. Med. 19 (2008) 3123–3133.
[20] Y. Zhang, J.D. Santos, Microstructural characterization and in vitro apatite formation in CaO–P_2O_5–TiO_2–MgO–Na_2O glass–ceramics, J. Eur. Ceram. Soc. 21 (2001) 169–175.
[21] A. Bigi, G. Falini, E. Foresti, M. Gazzano, A. Ripamonti, N. Roveri, Magnesium influence on hydroxy apatite crystallization, J. Inorg. Biochem. 49 (1993) 69–78.
[22] K.H. Karlsson, H.O. Ylanen, Porous bone implants, materials in clinical applications, in: P. Vincenzini (Ed.), 9th Cimtec-World Forum on New Materials, Florence, Italy, Advances in Science and Technology 33 (1998) 28.
[23] S. Yuzhen, S. Youan, H. Baoye, Influence of the mixed alkali effect on the chemical durability of Na_2O–TiO_2–SiO_2 glasses, J. Non-Cryst. Solids 80 (1986) 335–340.

[24] S. Pina, P.M. Torres, F. Goetz-Neunhoeffer, J. Neubauer, J.M.F. Ferreira, Newly developed Sr-substituted a-TCP bone cements, Acta Biomater. 6 (2010) 928–935.
[25] O.P. Filho, G.P. La Torre, L.L. Hench, Effect of crystallization on apatite layer formation on bioactive glass 45S5, J. Biomed. Mater. Res. 30 (1996) 509–514.
[26] J.R. Jones, P. Sepulveda, L.L. Hench, Dose-dependent behavior of bioactive glass dissolution, J. Biomed. Mater. Res. 58 (2001) 720–726.
[27] R.Z. LeGeros, O.R. Trautz, E. Klein, J.P Legeros, 2 Types of carbonate substitution in 560 apatite structure, Experientia 25 (1969) 5–7.
[28] J. Serra, P. Gonzalez, S. Liste, C. Serra, S. Chiussi, B. Leon, M. Pérez-Amor, H.O. Ylänen, M. Hupa, FTIR and XPS studies of bioactive silica based glasses, J. Non Cryst. Solids 332 (2003) 20–27.
[29] X. Lu, Y. Leng, Theoretical analysis of calcium phosphate precipitation in simulated body fluid, Biomaterials 26 (2005) 1097–1108.